applied sciences

MDPI

Article

Theoretical Exposure Dose Modeling and Phase Modulation to Pattern a VLS Plane Grating with Variable-Period Scanning Beam Interference Lithography

Ying Song [1], Ning Zhang [2], Yujuan Liu [1,*], Liu Zhang [1] and Zhaowu Liu [2]

[1] College of Instrumentation and Electrical Engineering, Jilin University, Changchun 130012, China
[2] Changchun Institute of Optics, Fine Mechanics and Physics, Chinese Academy of Sciences, Changchun 130033, China
* Correspondence: liuyujuan@jlu.edu.cn

Abstract: Variable-period scanning beam interference lithography (VP-SBIL) can be used to fabricate varied-line-spacing (VLS) plane gratings. The exposure phase modulation method to pattern a VLS grating with a desired groove density must be carefully devised. In this paper, a mathematical model of the total exposure dose for VLS plane grating fabrication is established. With model-based numerical calculations, the phase modulation effects of the parameters, including the fringe locked phase, fringe density, and step size, are analyzed. The parameter combinations for the phase modulation are compared and chosen, and the optimal coordinate for phase compensation is selected. The calculation results show that the theoretical errors of the groove density coefficients can be controlled within 1e-8. The mathematical model can represent the deposited exposure dose for patterning VLS gratings during the lithography process, and the chosen parameters and proposed phase modulation method are appropriate for patterning VLS gratings with VP-SBIL.

Keywords: varied-line-spacing (VLS) grating; exposure phase modulation; variable-period scanning beam interference lithography (VP-SBIL); phase compensation

Citation: Song, Y.; Zhang, N.; Liu, Y.; Zhang, L.; Liu, Z. Theoretical Exposure Dose Modeling and Phase Modulation to Pattern a VLS Plane Grating with Variable-Period Scanning Beam Interference Lithography. *Appl. Sci.* **2022**, *12*, 7946. https://doi.org/10.3390/app12157946

Academic Editor: Soshu Kirihara

Received: 3 June 2022
Accepted: 5 August 2022
Published: 8 August 2022

1. Introduction

A varied-line-spacing (VLS) plane grating is a straight groove periodic structure with a desired groove density function. VLS plane grating can self-focus and reduce aberration. The efficiency and resolving power of instruments can be improved. Compared with the concave grating, the substrate is easy to process. VLS plane gratings are widely used as key components in extreme ultraviolet spectrum analysis, monochromators, spectral imaging, and position sensors [1–6].

The most popular methods to pattern VLS plane gratings are diamond ruling, holographic imaging, and electron or laser beam lithography. Traditional direct-write methods such as diamond ruling and electron-beam or laser beam lithography can be extremely slow and expensive, and result in gratings with undesired phase errors [1,2,7]. Holographic gratings written by two-beam interference introduced a cost-effective path to more rapidly produce gratings with smoother phases. However, holographic methods require spherical or aspheric wavefront recording optics. The desired groove density frequently has difficulty satisfying geometrical constraints in spherical wavefront recording systems, and groove bending decreases the spectral resolution of the grating. Aspheric wavefront recording optics are complicated to design, manufacture, and align. The deviation and error from the recording optics introduce errors into the groove density distribution [8,9].

A variable-period scanning beam interference lithography (VP-SBIL) system is an effective tool to pattern high-fidelity general periodic structures in one or two dimensions within a short period. The VP-SBIL system uses small Gaussian beams with diameters of several micrometers to millimeters to form fringes in a small interference image. The

image has a very high phase fidelity. The fringe period and orientation can be progressively changed in a desirable fashion. The fringe phase can be locked using a high-bandwidth fringe locking system. The grating substrate is scanned under the image using a high-performance stage. A uniform exposure dose is achieved by overlapping the subsequent scans. The patterning process is fast and cost-effective because the interference image contains several hundred or thousands of fringes, and expensive aspheric optics are not required in VP-SBIL [10–12].

Fabricating a VLS grating with VP-SBIL is not as straightforward as the direct-write method. The groove density of the grating represents the grating phase distribution, which is determined by the exposure phase modulation. To fabricate a straight groove VLS grating using VP-SBIL, three questions must be answered. First, how to express the total exposure dose for patterning a VLS grating with VP-SBIL? Second, which parameters are chosen for the exposure phase modulation? Third, how to cooperatively regulate these parameters to acquire the desired phase distribution? In the published articles about VP-SBIL, the optical topology and basic manufacturing principle for variable-period structures are illustrated. However, details about the phase modulation are not mentioned [10–12]. We attempt to provide possible and simple answers to these questions. This is a key issue for practical applications of VP-SBIL [13–15].

This paper establishes a model of the total exposure dose for a VLS plane grating patterned with VP-SBIL. The exposure phase distribution and exposure contrast in an intuitive manner are verified, and the phase modulation effects of the parameters are given. The parameter selection for the phase modulation and the optimal coordinate for phase compensation to pattern the VLS grating are proposed. The results for an actual VLS plane grating are given. Finally, the reasons for the differences in the phase modulation performance and phase compensation are discussed.

2. Model of the Total Exposure Dose for VLS Grating Patterning

The desired groove density function of the VLS plane grating without higher-order aberration compensation can be expressed as follows

$$g(x) = n_{g0} + n_{g1}(x - W_g/2) \tag{1}$$

The desired phase variation of the VLS grating can be expressed as

$$\begin{aligned} \Phi_g(x) &= 2\pi \int_0^x g(x)dx \\ &= 2\pi\left[(n_{g1}/2)x^2 + (n_{g0} - n_{g1}W_g/2)x\right] \end{aligned} \tag{2}$$

where the x coordinate is along the vector direction of the grating. It is assumed that $x = 0$ is at the margin of the grating substrate. W_g is the grating width along the x-axis; n_{g0} is the groove density in the center of the grating with units of L/mm; n_{g1} is the slope with units of L/mm^2; and n_{g0} and n_{g1} are determined according to the aberration correction principle of the VLS grating and the structure of the spectrometer or the device, respectively.

In the VP-SBIL system, the step direction is along the x-axis, and the scanning direction is along the y-axis, which is parallel to the fringe direction. In this paper, the VLS grating was patterned with substrate parallel scanning. At the end of a scan, the stage stepped over and reversed direction for a new scan. The exposure phase was modulated during the step process, and the phase relative to the substrate remained unchanged during scanning. Other written modes such as Doppler scanning are not described here [16,17].

Let us assume a perfect stage scan, fringe period regulation, and fringe phase locking. The initial scan is at $x = X_0 = 0$. The fringe density in the initial scan is f_0. The dose delivered to the resist can be mathematically written as

$$D_0(x) = B(x) + A(x)\cos(2\pi x \cdot f_0 + \delta_0) \tag{3}$$

where $B(x)$ is the background dose. δ_0 is the locked phase introduced by the fringe locking unit in the initial scan. $A(x)$ is the normalized Gaussian dose amplitude in the x-direction and is expressed as

$$A(x) = \exp(-2x^2/\omega^2) \tag{4}$$

where ω is the $1/e^2$ radius of the Gaussian intensity envelope [16,17].

A uniform exposure dose is achieved by overlapping subsequent scans. After the first step with a step size S_1, $x = X_1 = S_1$ and its serial number $k = 1$. The dose deposited by the second scan ($k = 1$) is expressed as

$$D_1(x) = B(x - X_1) + A(x - X_1)\cos[2\pi \cdot f_1 \cdot (x - X_1) + \delta_1] \tag{5}$$

where f_1 is the fringe density in the second scan, and δ_1 is the phase introduced by the fringe locking unit.

Similarly, the exposure dose deposited by the $(k + 1)$-th scan after k steps ($k \geq 1$) is equal to the initial dose, but it has shifted in position due to the discrete stepping of the stage, which can be expressed with Equation (6). This is illustrated in Figure 1 (the fringe density is exaggerated for clarity).

$$D_k(x) = B(x - X_k) + A(x - X_k)\cos[2\pi f_k \cdot (x - X_k) + \delta_k] \tag{6}$$

where S_k is the k-th step size. The $(k + 1)$-th scan is at $x = X_k = \sum_{i=1}^{k} S_i$ after k steps. f_k and δ_k are the fringe density and locked phase introduced by the fringe locking unit in the $(k + 1)$-th scan, respectively.

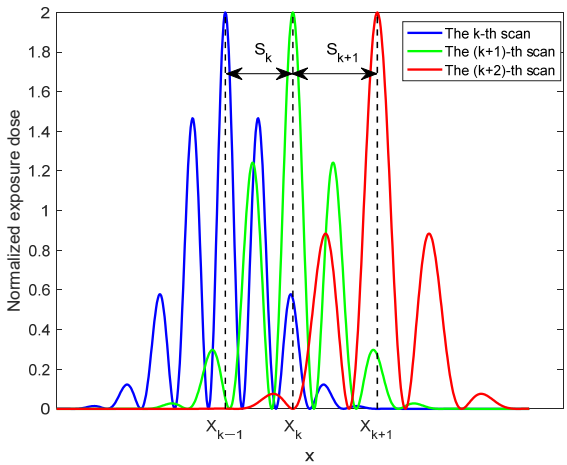

Figure 1. The exposure doses in three adjacent scans.

f_k ($k \geq 1$) can be written as $f_k = f_{k-1} + \Delta_k = f_0 + \sum_{i=1}^{k} \Delta_i$, where Δ_k is the density increment between the $(k + 1)$-th scan and the k-th scan. Equation (6) can be rewritten as

$$D_k(x) = B(x - X_k) + A(x - X_k)\cos(2\pi f_0 x + \varphi_k) \tag{7}$$

where φ_k is the phase increment between the $(k + 1)$-th scan and the initial scan, which can be expressed as

$$\varphi_k(x) = 2\pi\left(x\sum_{i=1}^{k}\Delta_i - f_0 X_k - X_k\sum_{i=1}^{k}\Delta_i\right) + \delta_k \tag{8}$$

From Equation (8), the phase increment between the $(k + 1)$-th scan and k-th scan can be expressed as

$$\varphi_{kd}(x) = \varphi_k(x) - \varphi_{k-1}(x) = \varphi_{kdx}(x) + \varphi_{kdc} + (\delta_k - \delta_{k-1}) \tag{9}$$

where $\varphi_{kdx}(x)$ is the term varying with x, $\varphi_{kdx}(x) = 2\pi x\Delta_k$. φ_{kdc} is the term independent of x. $\varphi_{kdc} = -2\pi\,(X_{k-1}\Delta_k + S_k f_k)$.

The resist on the substrate is deposited after N steps and $N + 1$ scans. The total exposure dose in the resist is the sum of all individual doses and can be expressed as

$$\begin{aligned} D_T(x) &= D_0(x) + D_1(x) + \cdots D_N(x) \\ &= D_{TB}(x) + A_T(x)\cos\Psi_T(x) \end{aligned} \tag{10}$$

where $D_{TB}(x)$ is the total background dose, $A_T(x)$ is the total dose amplitude, and $\Psi_T(x)$ is the exposure phase distribution. They can be expressed with Equations (11) and (12).

$$D_{TB}(x) = B(x) + B(x - X_1) + \cdots B(x - X_k) \tag{11}$$

$$\begin{aligned} A_T(x)\cos\Psi_T(x) &= A(x)\cos(2\pi f_0 x + \varphi_0) + A(x - X_1)\cos(2\pi f_0 x + \varphi_1) \\ &\quad + A(x - X_N)\cos(2\pi f_0 x + \varphi_N) \end{aligned} \tag{12}$$

From Equation (12), $A_T(x)$ and $\Psi_T(x)$ can be expressed as

$$\begin{cases} A_T(x) = \sqrt{E(x)^2 + F(x)^2} \\ \Psi_T(x) = 2\pi x f_0 + \Psi(x) \\ \Psi(x) = \arctan[F(x)/E(x)] \\ E(x) = A(x)\cos\varphi_0 + A(x - X_1)\cos\varphi_1 + \cdots A(x - X_N)\cos\varphi_N \\ F(x) = A(x)\sin\varphi_0 + A(x - X_1)\sin\varphi_1 + \cdots A(x - X_N)\sin\varphi_N \end{cases} \tag{13}$$

Let us assume that the resist on the substrate is uniform and linear to the exposure dose. $\Psi_T(x)$ determines the theoretical phase distribution of the fabricated grating. The phase error between the fabricated grating and the desired grating can be expressed as

$$\Phi_e(x) = \Psi_T(x) - \Phi_g(x) \tag{14}$$

The patterned grating with the desired $g(x)$ can be acquired under the condition of $\Phi_e(x) = 0$, which is the goal of the phase modulation. The total exposure contrast can be expressed as

$$\gamma(x) = A_T(x)/D_{TB}(x) \tag{15}$$

Equations (10)–(13) are the mathematical exposure dose model for the VLS grating exposure with VP-SBIL in the parallel scanning style. If f_k is constant in all scans, the dose model coincides with that in equal-period SBIL (EP-SBIL) [18,19].

3. Phase Modulation Effects of the Parameters and Parameter Selection

3.1. General Parameters and Numerical Calculation

As shown in Equations (8) and (13), $\Psi_T(x)$ is mainly determined by the locked phase δ_k, fringe density f_k, and step size S_k from all of the scans. Fortunately, all of these parameters can be adjusted in a VP-SBIL system. However, $\Psi_T(x)$ cannot be expressed with a simple mathematical form. It is difficult to directly solve the equation $\Phi_e(x) = 0$. The numerical calculation based on the exposure model is an effective means of analysis.

For simplicity, assume that the contrast in a single scan is 1, which implies that $A\,(x) = B\,(x)$ in Equation (3). A grating in a surface physics beamline monochromator is taken as an example. The parameters of the grating are W_g = 30 mm, n_{g0} = 1200 L/mm, and $n_{g1} = -0.7783$ L/mm^2 [20]. To avoid fringe smearing in VP-SBIL, a spot diameter in the range of 10–100 microns is optimal [11]. We chose ω = 100 μm for the numerical calculation and analysis. To achieve a uniform exposure dose, the adjacent scans overlap. As described in previous research on EP-SBIL, the step size is smaller, the uniformity and contrast decrease caused by phase error are better, but the exposure is slower. If the fringe period is constant in all scans, a step size of 0.9 times the $1/e^2$ radius (StepRatio = S_k/ω = 0.9) produces a better dose uniformity than 1% [18,19]. VLS grating fabrication requires fringe phase modulation in each step process, which implies that phase inconsistency in the

adjacent scans is inevitable. The step size should decrease with increasing the coefficient n_{g1} to satisfy the exposure contrast demand. As StepRatio is not a crucial parameter for phase modulation, we arbitrarily chose StepRatio = 0.8 for the small n_{g1} value in this paper.

With the above general parameters, the numerical calculation was developed with Matlab. To minimize the numerical artifact that may arise from an abrupt data cutoff, the total step-scan width W_t is larger than W_g ($W_t = W_g + 1$ mm), and a sufficiently wide x range [-5 mm, $W_t + 5$ mm] is chosen for calculation. To guarantee calculation precision, the calculation step is taken to be $1/100$ times ω. Based on the exposure model, the exposure doses are calculated and accumulated step by step in the same way as those in a real exposure process, and $\phi_e(x)$ and $\gamma(x)$ are calculated according to Equations (14) and (15). Because of the lack of sufficient overlap at the start and end scan segments, the data from $x = 0$ to $x = W_g$ are the focus. To observe the effect of δ_k, f_k, and S_k on $\Psi_T(x)$, three phase modulation manners by varying these parameters in an intuitive way with other parameters remaining unchanged are demonstrated. These approaches appeared to be feasible and needed to be verified, and the modulation effects of the parameters were analyzed. According to the numerical calculation results, the parameters for phase modulation were chosen.

3.2. Phase Modulation Effects of the Parameters

3.2.1. Phase Modulation by Varying Only δ_k

Set the fringe density to a constant value of $f_k = f_0 = n_{g0} - n_{g1} W_g/2$. It is equal to the desired density at $x = 0$. The step size is an integral multiple of the fringe period as that in a traditional EP-SBIL, which implies that $S_k = N_{steps}/f_0$ and $X_k = kN_{steps}/f_0$. N_{steps} influences the dose uniformity and exposure contrast. For general VLS gratings with a small coefficient n_{g1}, the grating density is mainly determined by n_{g0}. Therefore, N_{steps} is chosen as a constant expressed as

$$N_{steps} = round(\omega \cdot StepRatio \cdot n_{g0}) \tag{16}$$

Under these conditions, Equation (8) changes to a simple form $\varphi_k(x) = \delta_k$. If δ_k is used for phase modulation, all fringes in the image have identical phase variations, which implies that δ_k cannot be expressed as a function of the x coordinate.

1. Intuitively varying δ_k according to $\phi_g(x)$

Intuitively, changing the δ_k value with the desired ϕ_g phase in the $(k + 1)$-th scan appears to be feasible, which can be written as

$$\delta_k = \Phi_g(X_k) = 2\pi\left[(n_{g1}/2)X_k{}^2 + (n_{g0} - n_{g1}W_g/2)X_k\right] \tag{17}$$

$\phi_e(x)$ is shown in Figure 2, and it is basically piecewise linear with a transition region between the two adjacent linear segments. The exposure contrast is shown in Figure 3. The troughs of the exposure are in contrast with an amplitude close to zero. We performed a differential operation to $\phi_e(x)$. The differences in $\phi_e(x)$ are also shown in Figure 3. The x coordinates of the cusps in $\phi_e(x)$ coincide with those of the lowest contrasts. The frequency components of the exposure contrast are extracted using FFT (Fast Fourier Transform). Two main frequency components are approximately located at $F_{p1} = |0.5n_{g1}|/(2\pi)$ and $F_{p2} = 1/S_k$. The F_{p1} component is influenced by the linear variation of the grating density. The F_{p2} component is caused by the phase inconsistency in adjacent scans, which also exists in $\phi_e(x)$, as shown in Figure 3. $\phi_e(x)$ and $\gamma(x)$ cannot satisfy the demands of grating fabrication.

2. Phase modulation effect by only varying δ_k according to X_k

To modulate the phase by only varying δ_k, δ_k is different at different X_k. As shown in Equation (2), the desired phase variation is a quadratic polynomial. More generally, δ_k can be written in an analogous form expressed as

$$\delta_k = 2\pi\left(a_{\delta 2}X_k{}^2 + a_{\delta 1}X_k + a_{\delta 0}\right) \tag{18}$$

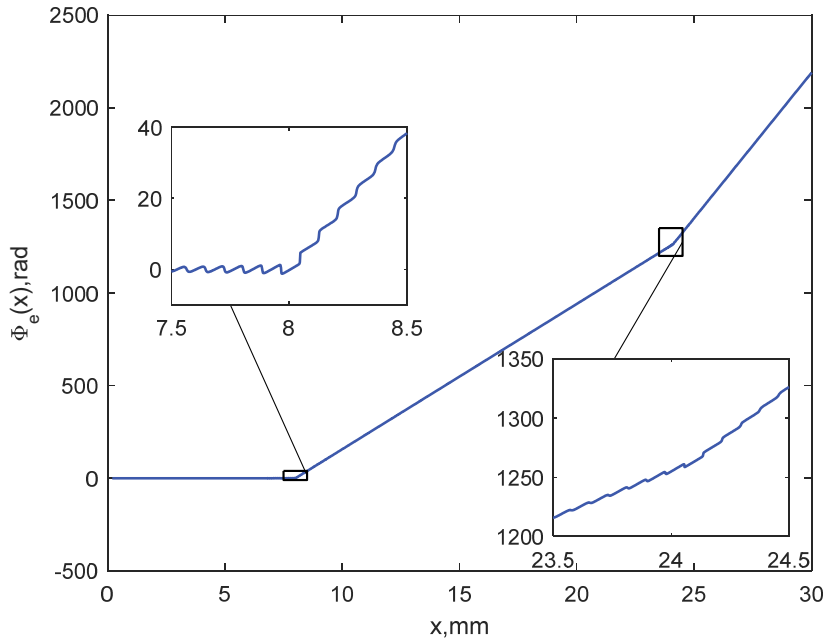

Figure 2. Phase error under the condition $\delta_k = \phi_g(X_k)$.

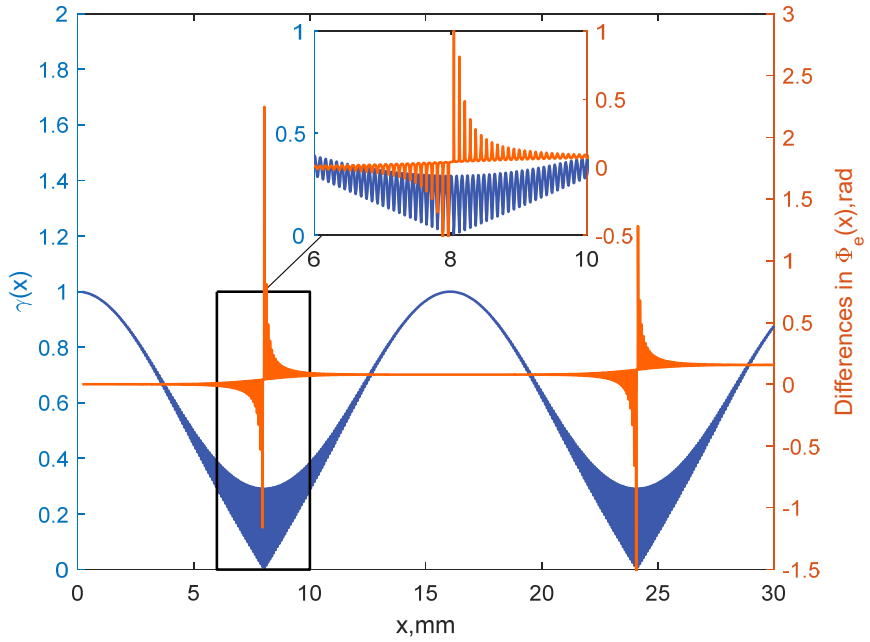

Figure 3. Exposure contrast and difference in $\phi_e(x)$ under the condition $\delta_k = \phi_g(X_k)$.

Through numerical calculation and theoretical analysis, the modulation effects of δ_k are as follows.

(1) $a_{\delta 2} = a_{\delta 1} = 0$, and $\varphi_k = \delta_c = 2\pi a_{\delta 0}$. The phase increments are constant for all scans. From Equation (13), $\Psi_T(x)$ can be expressed as

$$\Psi_T(x) = 2\pi f_0 x + \delta_c \tag{19}$$

The patterned grating is an equal-period grating with density f_0. The constant phase shift introduced by δ_c does not affect the grating characteristics. From Equation (15), $\gamma(x) = 1$.

(2) $a_{\delta 2} = 0$, $\varphi_k = \delta_k = 2\pi\,(a_{\delta 1} X_k + a_{\delta 0})$. $\Psi_T(x)$ is a linear function with the $F_{\mathrm{p}2}$ frequency component. The slope is influenced by $a_{\delta 1}$, and the constant term and $\gamma(x)$ are determined by $a_{\delta 1}$ and $a_{\delta 0}$. If the absolute value of $a_{\delta 1}$ is small, the slope of $\Psi_T(x)$ is approximately

$2\pi\ (f_0 + a_{\delta 1})$, which implies that $a_{\delta 1}$ can be used to change the period of the patterned grating. This conclusion is consistent with the phenomenon found in an EP-SBIL in Ref. [21]. $\gamma(x)$ is an average exposure contrast plus an $F_{\mathrm{p}2}$ frequency component. With a constant step size and small $a_{\delta 1}$, $a_{\delta 1}$ is smaller, the average exposure contrast is higher, and the amplitude of the $F_{\mathrm{p}2}$ component is smaller. With the general parameters for numerical calculation, the average $\gamma(x)$ is better than 0.9 when $|a_{\delta 1}| < 1.4$. To maintain the exposure contrast, the adjustment range of the grating density is limited to ± 1.4 L/mm.

(3) $a_{\delta 2} \neq 0$, $a_{\delta 1} \neq 0$ and $a_{\delta 0} \neq 0$. $\Psi_T(x)$ and $\phi_e(x)$ are basically piecewise quadratic polynomials. δ_k expressed with Equation (17) is a special case of this situation. $\phi_e(x)$ in Figure 2 is the piecewise quadratic with a quadratic coefficient of zero. The results are similar to those in Figures 2 and 3. $\phi_e(x)$ increases with x, and $\gamma(x)$ fluctuates between 0 and 1. The cusps of $\phi_e(x)$ and the lowest $\gamma(x)$ are located at the same x coordinates, and their spatial frequency is $|a_{\delta 2}|/(2\pi)$. There is also the $F_{\mathrm{p}2}$ frequency component caused by the phase inconsistency in the adjacent scans.

In other words, the desired VLS grating cannot be obtained by only varying δ_k in the form in Equation (18). δ_k can compensate for a certain phase error or change the density of an equal-period grating in a small range.

3.2.2. Phase Modulation by Varying f_k and δ_k

Instinctively, the VLS grating can be patterned by directly varying the fringe period according to $g(x)$. In the $(k+1)$-th scan, f_k is set to the desired density $g(X_k)$ of this scan, and $\Delta_k = f_k - f_{k-1} = n_{g1} S_k$. S_k is not used to modulate the phase in this manner. We chose a constant value of S_c = StepRatio·ω, and $X_k = kS_c$.

The unequal fringe density in the adjacent scans introduces the phase inconsistency. As described in Section 3.2.1, δ_k cannot compensate for the phase error varying with x. However, with δ_k in Equation (20), the fringe phase difference between the $(k+1)$-th scan and the k-th scan at a certain x_{comk} coordinate can be compensated.

$$\delta_k = \delta_{k-1} - \varphi_{kdx}(x_{comk}) - \varphi_{kdc} \tag{20}$$

With $f_0 = n_{g0} - n_{g1} W_g/2$, $\phi_{\mathrm{e}}(x)$ with different δ_k are shown in Figure 4. $\phi_e(x)$ is generally a piecewise quadratic polynomial with $\delta_k = 0$ or $\delta_k = \delta_{k-1} - \varphi_{kdc}$. The x coordinates of the cusps in $\phi_e(x)$ coincide with those of the lowest contrasts. $\phi_e(x)$ with $x_{comk} = (X_k + X_{k-1})/2$ is close to 0, and $\phi_e(x)$ with $x_{comk} = X_k$ and $x_{comk} = X_{k-1}$ have a cumulative characteristic. For small VLS gratings, the cumulative effects can be neglected. However, with increasing the grating size, the cumulative $\Phi_e(x)$ may have a great impact. The $F_{\mathrm{p}2}$ frequency component in $\phi_e(x)$ can be acquired by removing the linear polynomial from $\phi_e(x)$, as shown in Figure 5. The $F_{\mathrm{p}2}$ frequency components indicate that the phase inconsistences in the adjacent scans are not fully compensated. The peak-to-valley amplitude of the phase fluctuation is close to 2×10^{-4} rad, which is smaller than 1/30,000 groove period. The grating groove position error caused by the phase fluctuation is smaller than 0.028 nm for the grating example. Compared with the phase errors in nanometer scale caused by the substrate and resist roughness, development, and metrology frame, this small phase fluctuation can usually be neglected for general VLS gratings.

We performed a quadratic polynomial fitting to $\Psi_T(x)$. The fitting polynomial can be expressed as

$$\begin{aligned} \Psi_{Tp}(x) &= 2\pi\left(a_{\Psi 2}x^2 + a_{\Psi 1}x + a_{\Psi 0}\right) \\ &= 2\pi\int_0^x g_p(x)dx + \Psi_{Tp0} \end{aligned} \tag{21}$$

where $g_p(x) = n_{gp0} + n_{gp1}(x - W_g/2)$ can be treated as the theoretical groove density of the patterned grating. $\Psi_{Tp0} = 2\pi a_{\Psi 0}$ is the constant component of $\Psi_{Tp}(x)$, which has little effect on the characteristics of the grating. The groove density coefficients with different phase compensations are shown in Table 1. The theoretical groove densities $g_p(x)$ are close to the desired value, especially $g_p(x)$ with $x_{\mathrm{comk}} = (X_k + X_{k-1})/2$.

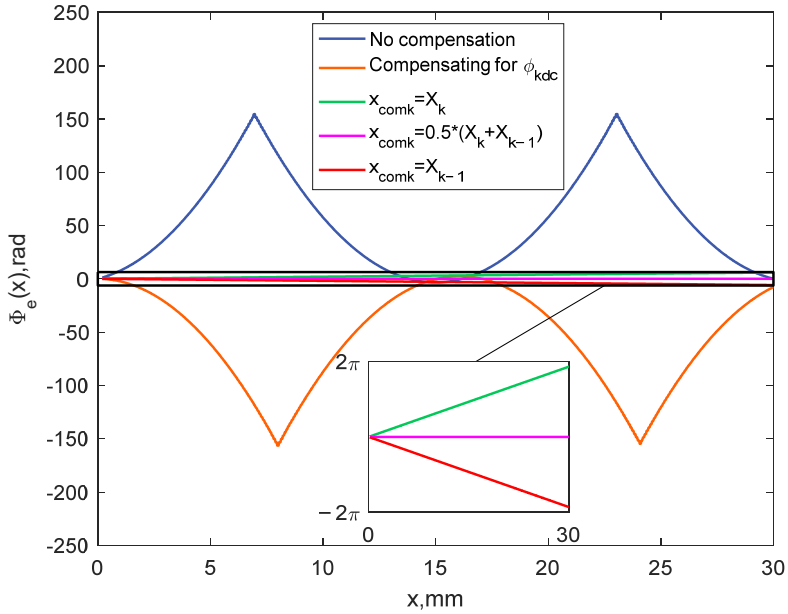

Figure 4. Phase error under the condition of $f_k = g(X_k)$ with different δ_k.

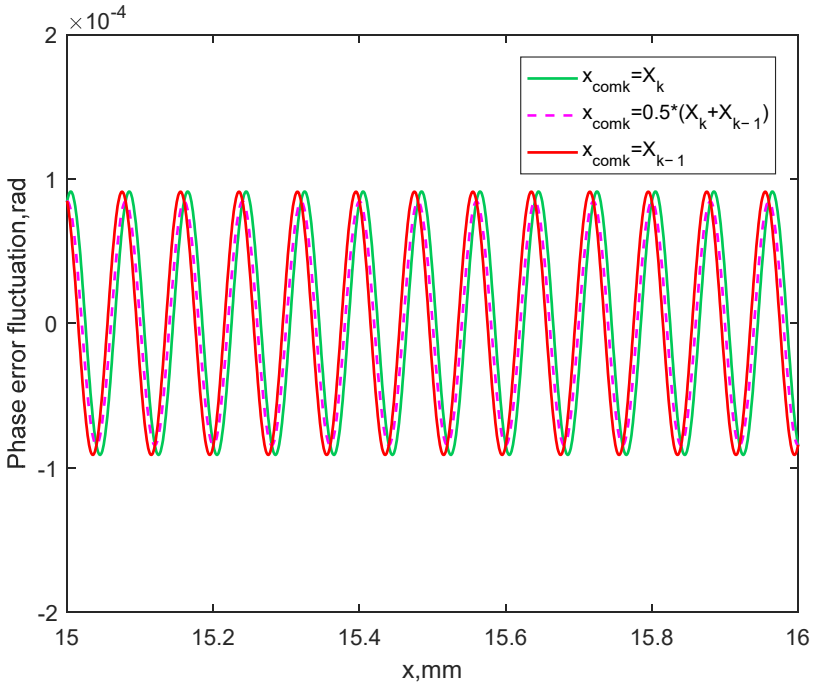

Figure 5. Phase error fluctuation under the condition of $f_k = g(X_k)$ with different δ_k.

Table 1. g_p(x) under the condition of $f_k = g(X_k)$ and phase compensation with δ_k.

x_{comk}	$g_p(x)$ Coefficients		Relative Errors of $g_p(x)$ Coefficients	
	n_{gp0}, L/mm	n_{gp1}, L/mm^2	$\varepsilon(n_{g0}) = \lvert n_{gp0} - n_{g0} \rvert / n_{g0}$	$\varepsilon(n_{g1}) = \lvert n_{gp1} - n_{g1} \rvert / n_{g1}$
X_k	1200.0311	−0.7783	2.5943×10^{-5}	$<1 \times 10^{-8}$
$(X_k + X_{k-1})/2$	1200.0000	−0.7783	$<1 \times 10^{-8}$	$<1 \times 10^{-8}$
X_{k-1}	1199.9689	−0.7783	-2.5943×10^{-5}	$<1 \times 10^{-8}$

The exposure contrasts $\gamma(x)$ are shown in Figure 6. The exposure contrasts are better than 0.99, and $\gamma(x)$ with $x_{comk} = (X_k + X_{k-1})/2$ is better than the others. The resist

has low-frequency filtering characteristics, so the influence of the F_{p2} fluctuation can be neglected [22,23]. The contrast can satisfy the demands of the grating exposure.

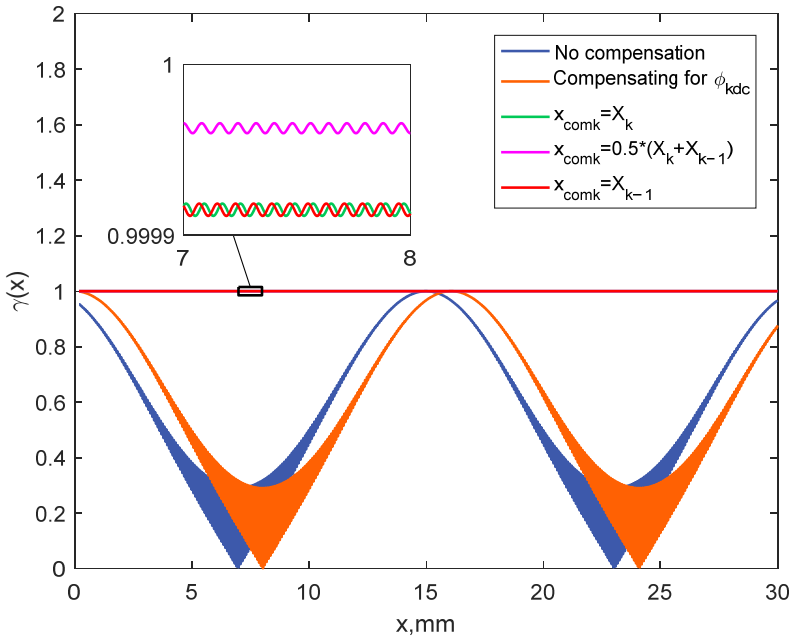

Figure 6. Exposure contrast under the condition of $f_k = g(X_k)$ with different δ_k.

3.2.3. Phase Modulation by Varying f_k, S_k and δ_k

The fringe density $f_k = g(X_k)$, and the step size S_k varies according to the fringe density. Here, we set S_k equal to an integer N_{steps} multiplied by a variable period value. N_{steps} is chosen to be the same constant expressed with Equation (16). The variable period value can be chosen as the fringe period in the adjacent last scan. S_k can be expressed as

$$S_k = N_{steps}/f_{k-1} \tag{22}$$

The phase difference can also be compensated with δ_k in Equation (20). With $f_0 = n_{g0} - n_{g1}W_g/2$ and the different phase compensation with δ_k, $\Phi_e(x)$ and $\gamma(x)$ are shown in Figures 7 and 8, respectively. Except for the condition of $\delta_k = \delta_{k-1} - \varphi_{kdc}$, $\Phi_e(x)$ is small, and the average contrasts are close to 1. The phase error from adjacent scans still causes F_{p2} fluctuations in $\Phi_e(x)$ and $\gamma(x)$.

As shown in Figure 7, $\Phi_e(x)$ with $\delta_k = 0$ is coincident with $\Phi_e(x)$ with $\delta_k = \delta_{k-1} - \varphi_{kdx}(X_k) - \varphi_{kdc}$, which implies that the step size expressed with Equation (22) can compensate for the phase difference at X_k. We assume that the phase difference at x_{comk} must be compensated, where x_{comk} is located between X_{k-1} and X_k. x_{comk} can be expressed with X_{k-1} and X_k as

$$x_{comk} = X_{k-1} + r(X_k - X_{k-1}) \tag{23}$$

where $r = (x_{comk} - X_{k-1})/(X_k - X_{k-1})$ is the ratio. If $\delta_k = 0$ for all scans, from Equations (9) and (23), the phase difference at x_{comk} in the k-th scan and $(k+1)$-th scan can be expressed as

$$\begin{aligned} \varphi_{kd}(x_{comk}) &= \varphi_{kdx}(x_{comk}) + \varphi_{kdc} \\ &= -2\pi S_k[(rf_{k-1} + (1-r)f_k)] \end{aligned} \tag{24}$$

From Equation (24), $\varphi_{kd}(x_{comk})$ can be compensated with S_k, expressed as

$$S_k = \frac{N_{steps}}{rf_{k-1} + (1-r)f_k} \tag{25}$$

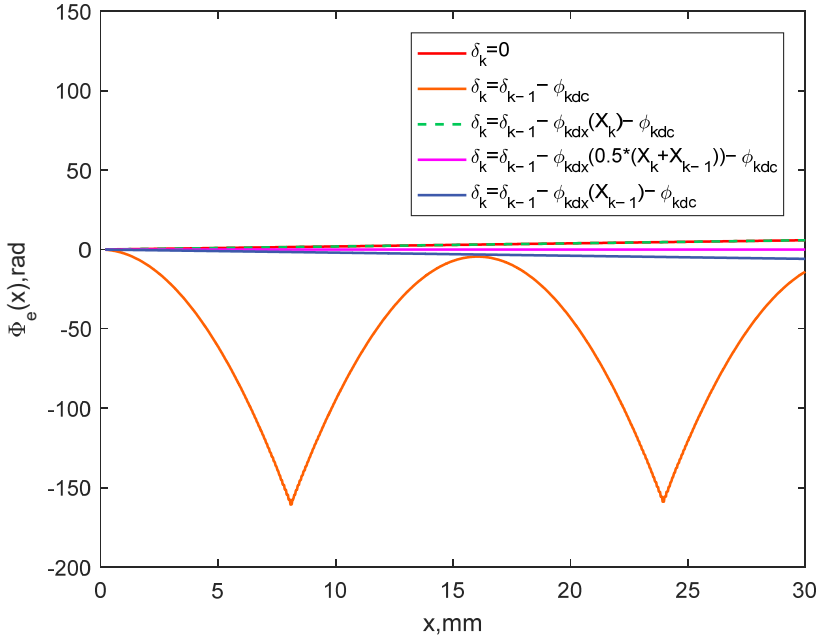

Figure 7. Phase error under the condition of $f_k = g(X_k)$ and $S_k = N_{steps}/f_{k-1}$ with different δ_k.

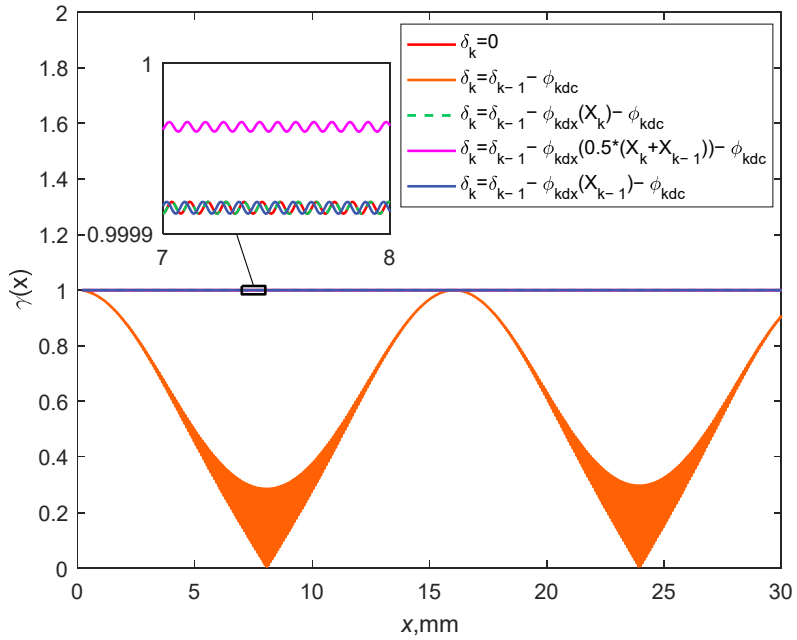

Figure 8. Exposure contrast under the condition of $f_k = g(X_k)$ and $S_k = N_{steps}/f_{k-1}$ with different δ_k.

If S_k is other values, such as an actual step size with a stage motion error, δ_k can be used for phase compensation, which implies that S_k and δ_k have similar phase modulation effects.

In this manner, the groove density coefficients with different phase compensations are shown in Table 2.

3.3. Parameter Selection for Phase Modulation

We demonstrate three intuitive phase modulation manners and analyze the phase modulation effects of the parameters, including the locked phase δ_k, fringe density f_k, and step size S_k. The results show that the desired phase distribution can be acquired by varying the parameter combinations as follows: (a) f_k and δ_k; (b) f_k and S_k; (c) f_k, S_k, and δ_k. These parameters can be selected for phase modulation.

Table 2. $g_p(x)$ under the condition of $f_k = g(X_k)$ and phase compensation with S_k.

x_{comk}	$g_p(x)$ Coefficients		Relative Errors of $g_p(x)$ Coefficients	
	n_{gp0}, L/mm	n_{gp1}, L/mm^2	$\varepsilon(n_{g0})$	$\varepsilon(n_{g1})$
X_k	1200.0311	−0.7783	2.5943×10^{-5}	-2.5946×10^{-5}
$(X_k + X_{k-1})/2$	1200.0000	−0.7783	$<1 \times 10^{-8}$	$<1 \times 10^{-8}$
X_{k-1}	1199.9689	−0.7783	-2.5943×10^{-5}	2.5946×10^{-5}

In an actual SBIL system, it is difficult to modulate the exposure phase by only varying S_k because of the stage positioning error. The stage positioning error can be corrected with δ_k according to the phase compensation relationship. Under this condition, an actual stage can be considered an ideal stage without a positioning error, similar to that in an EP-SBIL system. Therefore, parameter combinations (a) and (c) are applicable to practical applications. Comparing the groove density errors in Tables 1 and 2, the parameter combination (a) has a better performance, and $x_{comk} = (X_k + X_{k-1})/2$ is the optimal coordinate for phase compensation.

In addition to the grating example in Section 3.1, other VLS gratings, including another grating in a monochromator (n_{g0} = 400 L/mm, n_{g1} = −0.2594 L/mm and W_g = 80 mm) [20] and a grating in a diagnostic spectrometer (n_{g0} = 600 L/mm, n_{g1} = −0.7869 L/mm and W_g = 30 mm) [24], are designed for further verification. The results are consistent with the above results. Compared with the existing fabrication methods of VLS gratings, the relative errors of the groove density can satisfy the technical requirements [1–3,8,20,24], and the exposure contrast can satisfy the demands for VLS grating fabrication.

4. Discussion

Although S_k and δ_k have similar phase compensation effects, the results show that parameter combination (a) performs better, and $x_{comk} = (X_k + X_{k-1})/2$ is the optimal coordinate for phase compensation. The reason for the phenomenon will be discussed.

First, let us focus on the performance differences with different parameter combinations. In parameter combination (b) and (c), S_k varies with $f_{k-1,}$ as expressed in Equation (22). For the VLS grating example in this paper, S_k increases with k. With an increasing S_k, the phase inconsistency from adjacent scans has a greater impact on the phase error and exposure contrast. Therefore, the overall performances with parameter combination (b) and (c) decrease with increasing S_k, and a constant $S_k = S_c$ maintains a consistent performance with combination (a).

Second, the selection of x_{comk} and the cause of the cumulative characteristic in $\Phi_e(x)$ with $x_{comk} \neq (X_k + X_{k-1})/2$ are discussed. As shown in Equation (9), after the phase difference at x_{comk} is compensated with δ_k or S_k, the residual phase in $\varphi_{kdx}(x)$ is expressed as

$$\begin{aligned} \varphi_{kd\_res}(x) &= \varphi_{kdx}(x) - \varphi_{kdx}(x_{comk}) \\ &= 2\pi\Delta_k(x - x_{comk}) \end{aligned} \tag{26}$$

As shown in Figure 1, the overall phase compensation performance in the x range between X_{k-1} and X_k is mainly determined by the k-th scan and $(k+1)$-th scan. The overall phase compensation error can be estimated with the integral of $\varphi_{kd\_res}(x)$ in the range $[X_{k-1,}\ X_k]$ as

$$\begin{aligned} I_k(x_{comk}) &= \int_{X_{k-1}}^{X_k} \varphi_{kd\_res}(x)dx \\ &= 2\pi\Delta_k S_k[(X_k + X_{k-1})/2 - x_{comk}] \end{aligned} \tag{27}$$

Although Equation (27) is not a strict mathematical deduction based on the exposure model, it provides a tool for the analysis. The absolute value of I_k is smaller, and the phase compensation performance is better. If $x_{comk} = (X_k + X_{k-1})/2$, the best phase compensation performance can be obtained with $I_k = 0$, and it is not affected by S_k. Therefore, $(X_k + X_{k-1})/2$ is a good selection for x_{comk}. If $x_{comk} \neq (X_k + X_{k-1})/2$, the phase compensa-

tion performance degrades with $|I_k(x_{comk})| > 0$. As shown in Figures 4 and 7, $I_k(X_k)$ and $I_k(X_{k-1})$ have the same absolute value with opposite signs, which is consistent with the cumulative $\Phi_e(x)$ with different variation directions.

5. Conclusions

In this paper, a mathematical model of the total exposure dose for patterning a VLS grating with VP-SBIL is established, and the phase modulation method of the exposure is proposed. According to the model, the phase modulations in three intuitive manners are calculated, and the phase modulation effects of the parameters, including the locked phase, fringe density, and step size, are analyzed. The phase errors with phase compensation at different coordinates are compared and discussed, and the optimal coordinate for phase compensation is presented. The results show that three parameter combinations can be selected for phase modulation, and the phase modulation performance with the locked phase and the fringe density is better than those with other parameter combinations. The average value of the coordinates in two adjacent scans is the optimal coordinate for phase compensation. The theoretical error between the patterned grating and the desired grating can be controlled within 1e-8, and the requirements of the grating phase distribution and exposure contrast can be satisfied. The proposed exposure dose model and exposure phase modulation method are suitable for VLS planar grating fabrication with VP-SBIL.

Author Contributions: Conceptualization, Y.S. and N.Z.; software, Y.S.; validation, Y.L. and Z.L.; investigation, L.Z.; writing—original draft preparation, Y.S. and N.Z.; writing—review and editing, Y.L.; supervision, L.Z.; project administration, L.Z.; funding acquisition, Y.S., Y.L. and Z.L. All authors have read and agreed to the published version of the manuscript.

Funding: This research was funded by the National Natural Science Foundation of China (NSFC), grant numbers 61905243, 61905245, and 41974210; Scientific Research Project of Education Department of Jilin Province, grant number JJKH20220992KJ; Jilin Province Science and Technology Development Program Project in China, grant number 20200401071GX; and Natural Science Foundation of Jilin Province, grant number 20200201205JC.

Institutional Review Board Statement: Not applicable.

Informed Consent Statement: Not applicable.

Data Availability Statement: The data presented in this study are available on request from the corresponding author.

Acknowledgments: The authors would like to thank the Editor-in-Chief, Editor, and anonymous Reviewers for their valuable reviews.

Conflicts of Interest: The authors declare no conflict of interest.

References

1. He, W.; Zhang, W.; Meng, F.; Zhu, L. Electron beam lithography inscribed varied-line-spacing and uniform integrated reflective plane grating fabricated through line-by-line method. *Opt. Laser Eng.* **2021**, *138*, 106456. [CrossRef]
2. Voronov, D.L.; Warwick, T.; Gullikson, E.M.; Salmassi, F.; Naulleau, P.; Artemiev, N.A.; Lum, P.; Padmore, H.A. Variable line spacing diffraction grating fabricated by direct write lithography for synchrotron beamline applications. *Proc. SPIE* **2014**, *9207*, 920706.
3. Reininger, R.; de Castro, A.R.B. High resolution, large spectral range, in variable-included-angle soft X-ray monochromators using a plane VLS grating. *Nucl. Instrum. Methods Phys. Res. A* **2005**, *538*, 760–770. [CrossRef]
4. Pu, T.; Cao, F.; Liu, Z.; Xie, C. Deep learning for the design and characterization of high efficiency self-focusing grating. *Opt. Commun.* **2022**, *510*, 127951. [CrossRef]
5. Vannoni, M.; Martin, I.F. Absolute, high-accuracy characterization of a variable line spacing grating for the European XFEL soft X-ray monochromator. *Opt. Express* **2017**, *25*, 26519. [CrossRef] [PubMed]
6. Shimizu, Y.; Ishizuka, R.; Mano, K.; Kanda, Y.; Matsukuma, H.; Gao, W. An absolute surface encoder with a planar scale of variable periods. *Precis. Eng.* **2021**, *67*, 36–47. [CrossRef]
7. Koike, M.; Namioka, T. Plane grating for high-resolution grazing-incidence monochromators: Holographic grating versus mechanically ruled varied-line-spacing grating. *Appl. Opt.* **1997**, *36*, 6308–6318. [CrossRef] [PubMed]

8. Jiang, Y. The Research on Design Methods and Fabricating Technology of Varied Line-Space Holographic Plane Grating. Ph.D. Thesis, Chinese Academy of Sciences, Beijing China, 2015.
9. Wang, K.; Zheng, J.; Liu, Y.; Gao, H.; Zhuang, S. Electrically tunable two-dimensional holographic polymer-dispersed liquid crystal grating with variable period. *Opt. Commun.* **2017**, *392*, 128–134. [CrossRef]
10. Schattenburg, M.L.; Chang, C.H.; Heilmann, R.K.; Montoya, J.; Zhao, Y. Advanced interference lithography for Nanomanufacturing. *Int. Soc. Nanomanufacturing* **2006**, *44*, 441–445.
11. Schattenburg, M.L.; Chen, C.G.; Heilmann, R.K.; Konkola, P.T.; Pati, G.S. Progress towards a general grating patterning technology using phase-locked scanning beams. *Proc. SPIE* **2002**, *4485*, 378–384.
12. Pati, G.S.; Heilmann, R.K.; Konkola, P.T.; Joo, C.; Chen, C.G.; Murphy, E.; Schattenburg, M.L. Generalized scanning beam interference lithography system for patterning gratings with variable period progressions. *J. Vac. Sci. Technol. B* **2002**, *20*, 2617–2621. [CrossRef]
13. Song, Y.; Liu, Y.; Jiang, S.; Zhu, Y.; Zhang, L.; Liu, Z. Method for exposure dose monitoring and control in scanning beam interference lithography. *Appl. Opt.* **2021**, *60*, 2767–2774. [CrossRef] [PubMed]
14. Liu, Z.; Yang, H.; Li, Y.; Jiang, S.; Wang, W.; Song, Y.; Bayanheshig; Li, W. Active control technology of a diffraction grating wavefront by scanning beam interference lithography. *Opt. Express* **2021**, *29*, 37066. [CrossRef] [PubMed]
15. Jiang, S.; Lü, B.; Song, Y.; Liu, Z.; Wang, W.; Li, S.; Bayanheshig. Heterodyne period measurement in a scanning beam interference lithography system. *Appl. Opt.* **2020**, *59*, 5830–5836. [CrossRef] [PubMed]
16. Heilmann, R.K.; Konkola, P.T.; Chen, C.G.; Pati, G.S.; Schattenburg, M.L. Digital heterodyne interference fringe control system. *J. Vac. Sci. Technol. B.* **2001**, *19*, 2342–2346. [CrossRef]
17. Montoya, J. Toward Nano-Accuracy in Scanning Beam Interference Lithography. Ph.D. Thesis, Massachusetts Institute of Technology, Cambridge, MA, USA, 2006.
18. Chen, C.G. Beam Alignment and Image Metrology for Scanning Beam Interference Lithography: Fabricating Gratings with Nanometer Phase Accuracy. Ph.D. Thesis, Massachusetts Institute of Technology, Cambridge, MA, USA, 2003.
19. Konkola, P.T. Design and Analysis of a Scanning Beam Interference Lithography System for Patterning Gratings with Nanometer-Level Distortions. Ph.D. Thesis, Massachusetts Institute of Technology, Cambridge, MA, USA, 2003.
20. Li, C. Variable-Line-Spacing Grating Monochromators Design and Key Techniques. Ph.D. Thesis, University of Science and Technology of China, Hefei, China, 2014.
21. Jiang, S.; Bayanheshig; Li, W.; Song, Y.; Pan, M. Effect of period setting value on printed phase in scanning beam interference lithography system. *Acta Opt. Sin.* **2014**, *34*, 0905003. [CrossRef]
22. Dill, F.H.; Hornberger, W.P.; Hauge, P.S.; Shaw, J.M. Characterization of positive photoresist. *IEEE Trans. Electron Devices* **1975**, *22*, 445–452. [CrossRef]
23. Han, J.; Bayanheshig; Li, W.; Kong, P. Profile evolution of grating masks according to exposure dose and interference fringe contrast in the fabrication of holographic grating. *Acta Opt. Sin.* **2012**, *32*, 0305001. [CrossRef]
24. Jiang, Y.; Bayanheshig; Yang, S.; Zhao, X.; Wu, N.; Li, W. Study on the effects and compensation effect of recording parameters error on imaging performance of holographic grating in on-line spectral diagnose. *Spectrosc. Spectr. Anal.* **2016**, *36*, 857–863.